applied sciences

MDPI

Article

Trace Metal Partitioning in the Salinity Gradient of the Highly Stratified Estuary: A Case Study in the Krka River Estuary (Croatia)

Saša Marcinek *, Ana Marija Cindrić, Jasmin Pađan and Dario Omanović *

Center for Marine and Environmental Research, Ruđer Bošković Institute, 10000 Zagreb, Croatia; ana-marija.cindric@irb.hr (A.M.C.); jasminpadjan@gmail.com (J.P.)
* Correspondence: smarcin@irb.hr (S.M.); omanovic@irb.hr (D.O.)

Abstract: A size partitioning of several trace metals (Zn, Cd, Pb, Cu, Ni, Co, Mn, Fe and Al) between five size fractions (<3 kDa, 3 kDa–0.1 µm, 0.1 µm–1.2 µm, 1.2 µm–5 µm and >5 µm) was studied in the vertical salinity gradient of the highly stratified Krka River estuary. The results indicated a dominant river source for Zn, Co, Mn, Fe and Al and a diluting effect on Cd, Pb and Ni. The truly dissolved fraction (<3 kDa) dominated the Zn, Cd, Cu, Ni and Co pool, and a large part of Pb, Mn, Fe and Al was present in >5 µm particles. Pb, Mn, Fe and Al were closely related, showing a precipitation and colloidal aggregation in the surface layers and dissolution in the seawater layer. The highest percentage (30–37%) of colloids (3 kDa–0.1 µm) in the dissolved pool was found for Pb, Cu, Fe and Al. Differences in size distribution between low and high river flow periods revealed that Zn, Pb, Co, Mn, Fe and Al are introduced by the river mostly in the 3 kDa–5 µm size range. Therefore, a low percentage of colloidally bound metals compared to other coastal areas can be explained by a limited riverine input of terrigenous material, characteristic for this estuary. Correlation with PARAFAC components revealed associations of Cu with protein-like substances and Co with humic-like substances. The accumulation of Cu at the freshwater-seawater interface coupled with an increase of its colloidal fraction was observed, apparently governed by biologically produced organic ligands.

Keywords: trace metals; fractionation; colloids; truly dissolved; estuary

check for updates

Citation: Marcinek, S.; Cindrić, A.M.; Pađan, J.; Omanović, D. Trace Metal Partitioning in the Salinity Gradient of the Highly Stratified Estuary: A Case Study in the Krka River Estuary (Croatia). *Appl. Sci.* **2022**, *12*, 5816. https://doi.org/10.3390/app12125816

Academic Editors: Franz Saija, Ottavia Giuffrè, Giuseppe Cassone and Claudia Foti

Received: 25 May 2022
Accepted: 6 June 2022
Published: 8 June 2022

Publisher's Note: MDPI stays neutral with regard to jurisdictional claims in published maps and institutional affiliations.

Copyright: © 2022 by the authors. Licensee MDPI, Basel, Switzerland. This article is an open access article distributed under the terms and conditions of the Creative Commons Attribution (CC BY) license (https://creativecommons.org/licenses/by/4.0/).

1. Introduction

Trace metals in natural waters are distributed among various physical phases: particulate, colloidal and truly dissolved [1]. Dissolved and particulate metals are operationally separated with a 0.45 or 0.2 µm pore size filter, and the colloidal fraction is defined as having at least one dimension in the size range between 1 nm in diameter (which roughly equates with molecules of 1 kDa nominal molecular weight) and 1 µm [2–4]. The interactions among these phases appear to govern the fate and transport of the metals in the environment [5]. In coastal waters, especially in estuaries, processes affecting the trace metal speciation and fractionation play a key role in their transport to the open sea. Due to their large specific area, exposing a high number of reactive functional groups, colloidal particles play an important role in trace metal scavenging and thus control their cycling in coastal waters and their downward transport in the water column [5,6]. The estuarine reactivity of colloidal trace metals appears to be governed by their affinity for organic matter and for particulate surfaces [5]. Concentration and type of organic matter have a great influence on the aggregate formation and mobility of many trace metals (e.g., Zn, Pb, Cd, Cu, Ni and Co) in the estuaries. Due to their affinity to trace metals, organic ligands can control their size partitioning between solution and suspended particles and become the dominant carrier phase for these metals [7–10]. Besides organic matter, Mn- and Fe-rich colloids can act as the principal sorptive carrier phase for some trace elements in estuarine waters (e.g., As, Pb and Zn) [7,9]. Colloids play an important role in the exchange processes of

metals between the sediment and the water column [11]. The bridging of inorganic colloids by organic substances (humic substances and biopolymers) in an estuarine mixing area represents the major route for the aggregate formation and elimination of trace metals from the water column by sedimentation [3,12]. On the other hand, for some metals, distribution can be governed by the release from colloidal aggregates due to the competitive effects of major cations/anions (e.g., the formation of stable Cd chloro-complexes) [13–15]. While the aggregation is the main process causing the trace metal removal from the water column, the release of metals from particles during the sediment resuspension is the main counteractive process in the freshwater-seawater mixing area [16,17]. Additional various biotic and abiotic processes (e.g., metal biouptake, production of biogenic ligands, photodegradation or microbial degradation of organic matter, biological impact on metal deposition and remobilization from sediments) are of great importance for trace metal distribution and colloid formation/degradation within the estuary [16].

Most of the studies that were conducted in estuarine systems dealt with the particulate and dissolved fractions. However, separation of the dissolved from the particulate phase does not isolate colloids but rather includes them in the dissolved fraction. Colloids can be isolated by a variety of physicochemical techniques such as ultrafiltration, dialysis, gel techniques, field flow fractionation and capillary electrophoresis [6,18–22]. Among them, a low-cost and easily implemented technique, centrifugal ultrafiltration, is considered to be a high-efficiency colloidal substance separation technology [23,24].

The Krka River estuary is a very interesting system for the investigation of trace metal partitioning, since for most of the year it features a pristine environment with low organic content. Namely, due to the scarce vegetation, the absence of significant anthropogenic influence and self-purifying ability of the Krka River, the estuary, as well as the coastal sea, are unusually clean in terms of trace elements, terrigenous material and biomarkers [8,25–30]. The only concern presents the seasonal anthropogenic pressure related to increased boat traffic and touristic activities [8,31]. The estuary is permanently stratified: the surface fresh/brackish layer (FWL) is separated from the seawater layer (SWL) by a freshwater-seawater interface (FSI) formed at a depth between 1.5 and 5 m [8,30]. A strong and persistent halocline at the FSI is another interesting characteristic of the Krka River estuary. It prevents the exchange between the layers and acts as a physical barrier due to the difference in the density of water preventing the large part of sinking particles to settle down. The FSI is thus enriched with trace elements and nutrients, as well as with the dissolved, colloidal and particulate organic matter, including living and dead microorganisms [32–35].

In this study, the concentration and distribution of metals (Zn, Cd, Pb, Cu, Ni, Co, Mn, Fe and Al) between five size fractions with a close 'logarithmic' scale distribution (<3 kDa, 3 kDa–0.1 µm, 0.1 µm–1.2 µm, 1.2 µm–5 µm and >5 µm) were investigated along the vertical salinity gradient in the Krka River estuary. For this purpose, the syringe filtration technique and centrifugal ultrafiltration (for metals in the truly dissolved fraction: <3 kDa) were used in conjunction with acid extraction and stripping voltammetry and high resolution inductively coupled plasma mass spectrometry (HR-ICP-MS) as analytical techniques. Numerous studies have been performed in the Krka River estuary, including analysis of various trace metals in longitudinal transect as well as method-dependent (anodic stripping voltammetry and diffusive gradient in thin films) 'labile' metals in the vertical salinity gradient [8,27–29]. The aim of this work was to complement these studies with a preliminary exploration of trace metal size distribution and an evaluation of the importance of colloids to their behavior within the estuary, in which vertical salinity profiles were specifically analyzed. This pilot study should be the strong base for further research plans and in-depth analyses across the estuarine transect.

2. Materials and Methods

Six sampling campaigns were conducted in the Krka River estuary (Croatia) located in front of Šibenik town (N 43°44′9.509″, E 15°52′37.145″): 28 July 2018; 11 February

and 31 July 2019; 24 July and 20 September 2020; 7 April 2021. Samples of the vertical column profile were collected by a 'butterfly'-type vertical water sampler or van Dorn-type horizontal sampler (alfa or beta, Wildco) at 6 depths (M1–M6), selected according to the measured vertical salinity profiles (using the EXO2 multiparameter CTD probe, YSI, Yellow Springs, USA) and the total water column depth: M1 and M2 in FWL, M3 and M4 in FSI, M5 and M6 in SWL. Exact depths are readable in the vertical profiles of trace metals that are presented in Figure 1.

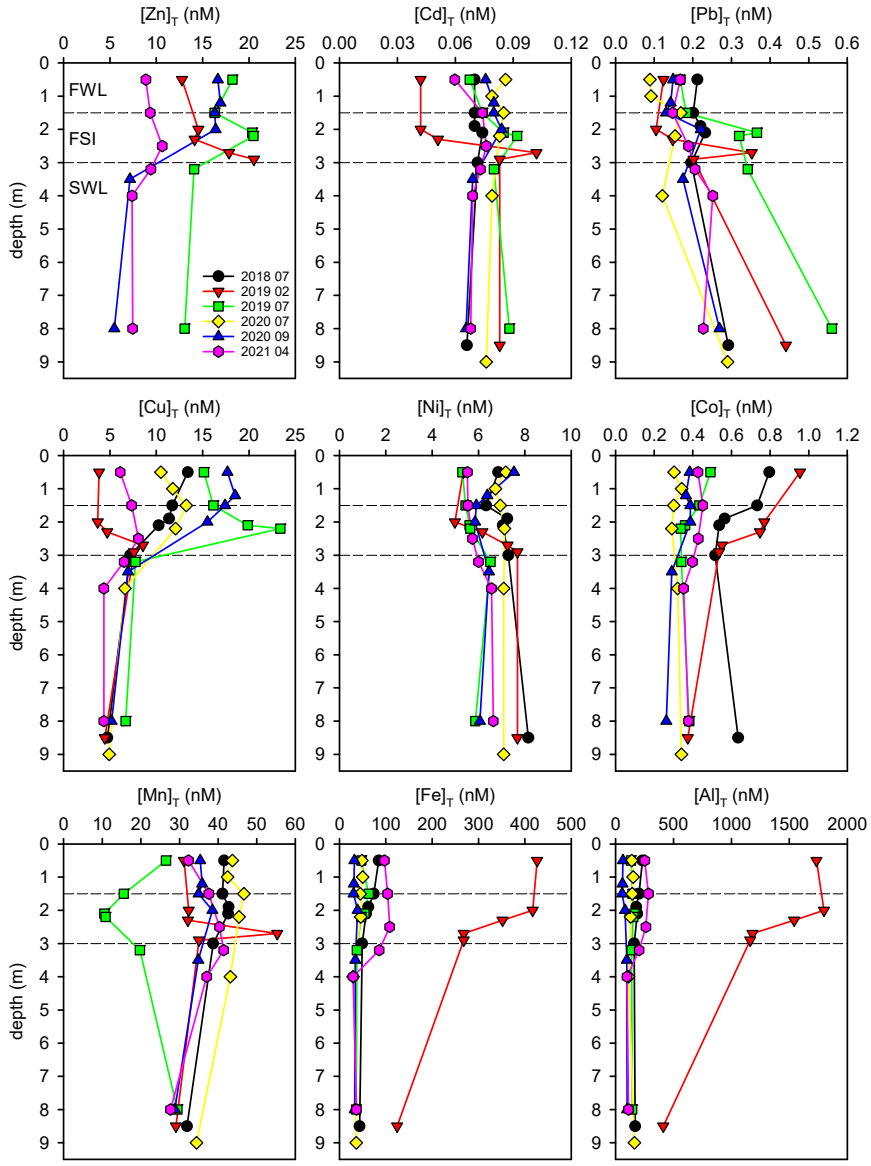

Figure 1. Depth profiles of the concentrations of studied trace metals in the total fraction (unfiltered sample). Dashed lines separate the three distinct layers, the freshwater layer (FWL), freshwater-seawater interface (FSI) and seawater layer (SWL), as indicated in the first graph.

After the sampling, samples were filtered using pre-cleaned cellulose-nitrate capsule filters of nominal pore sizes of 5, 1.2 and 0.1 µm (Minisart, Sartorius). The truly dissolved fraction was separated by centrifugal ultrafiltration (4000 rpm, 30 min; Eppendorf centrifuge, model 5804) through a polyethersulfone (PES) ultrafiltration membrane, with a nominal molecular weight of 3 kDa (Sartorius, Vivaspin 15 Turbo ultrafiltration spin columns). An ultrafiltered sample was obtained from the previously filtered sample using a 0.1 µm pore size. Repeated tests showed that the selected membrane and syringe filters were contamination free on trace metals, since the ultrapure (MilliQ) water (18.2 MΩ,

Synthesis A10, Millipore, Burlington, VT, USA) filtered through the pre-cleaned filters showed no difference in trace metal concentrations compared to the unfiltered MilliQ water. The ultrafiltration system, however, showed the gain of dissolved organic carbon and absorbance peak during filtration, even though PES was proposed as the best membrane material for the filtration of dissolved organic matter [36]. A possible source of dissolved organic carbon contamination is leaching from the polypropylene holder under the slightly increased temperature (up to 30 °C) during the centrifugation. Due to this reason, planned analysis separating the colloidal and truly dissolved organic matter was not possible.

Filtered and unfiltered samples were acidified by the addition of 0.2% v/v HNO_3 (69% w/w HNO_3 ROTIPURAN Supra, Carl Roth) to a pH < 2 and were UV-irradiated (250 W high pressure Hg lamp) for at least 24 h in order to decompose the natural organic matter. Samples were analyzed using stripping voltammetry (Zn, Cd, Pb, Cu, Ni and Co) and HR-ICP-MS (Zn, Cu, Mn, Fe and Al). A certified reference material "Nearshore seawater Reference Material for Trace Metals" CASS-5 (National Research Council of Canada) was used for validation of the analysis.

Voltametric measurements were carried out in a three-electrode cell (663 VA Stand, Metrohm, Herisau, Switzerland) controlled by Metrohm-Autolab (Eco Chemie, Utrecht, The Netherlands) potentiostat/galvanostat (μAutolab Type III or PGSTAT128N) in conjunction with the IME663 module (Metrohm-Autolab, Herisau, Switzerland) interfaced with a GPES (General Purpose Electrochemical System) v.4.9 software (Eco Chemie). The three-electrode system consisted of (i) a hanging mercury drop (HMDE; MME, Metrohm) (drop size 2:0.40 mm^2), serving as the working electrode, (ii) a Pt wire, serving as the counter electrode and (iii) a Ag | AgCl | sat. NaCl reference electrode. A home-made quartz electroanalytical cell with a working volume of 10–50 mL was used. In order to remove reactive dissolved oxygen, the sample (10–12 mL) was purged with nitrogen, for at least 3 min prior to the first measurement, and for 15–30 s between separate measurements in the same sample. During the measurement, a nitrogen blanket was maintained over the sample. Samples were added to the electrochemical cell by the in-house constructed autosampler, and the addition of standards was conducted by an automated burette system (Cavro XE 1000 or XL 3000 syringe pumps, Tecan, San Jose, CA, USA). The purpose-developed VoltAA (Voltammetric AutoAnalyser) software was used for the preparation of the project file for the GPES software and the data handling after the automated analysis. Concentrations of Cu, Cd, Pb, Zn, Ni and Co in filtered and unfiltered samples were determined by means of the standard addition (n = 4) method, using stripping voltammetry in differential pulse mode: anodic stripping voltammetry (DP-ASV) for Zn, Cd, Pb, and Cu, and adsorptive cathodic stripping voltammetry (DP-AdCSV) with Dimethylglyoxime as a complexing ligand for Ni and Co. The analysis was validated by repeated measurements (n = 7) of the UV-irradiated CASS-5. The determined metal concentrations (±standard deviation) were within the certified limits.

A magnetic sector field high resolution inductively coupled plasma mass spectrometer (HR-ICP-MS; Element 2, Thermo Scientific, Bremen, Germany) was used for multielemental analysis. Samples were diluted 10 times with 2% v/v HNO_3 *s.p.* to minimize the matrix effect linked to the presence of salt. Indium at a concentration of 10 μg L^{-1}, was used as an internal standard. The concentrations of elements were determined by means of using matrix matching (10× diluted UV-irradiated seawater) external calibrations. External calibration standards were prepared by dilution of the multi-element standard (NIST traceable) in 2% v/v HNO_3 *s.p.* at the following concentrations: 0, 0.1, 1 and 10 μg L^{-1}. CASS-5 was analyzed multiple times during the one sequence (n = 8). The obtained trace element concentrations (±standard deviation) were within the certified limits.

The measured trace metal concentrations in the unfiltered samples represent acid-leachable (quasi-total) metal concentrations, and within the text, they are referred to as total metal concentrations. Particulate and dissolved fractions are usually separated using 0.2 μm pore size filters, and for the separation of colloidal and truly dissolved fractions, membranes of nominal weight between 1–10 kDa are most frequently used [6,21,22,24,37].

In this work, the fraction >0.1 µm was considered as particulate and <3 kDa as truly dissolved, making the 3 kDa–0.1 µm size range a colloidal fraction. However, colloids are often components of complexed aggregates and can occur in sizes up to 1 µm. Therefore, colloids in the range between 0.1 µm and 1.2 µm were also considered, as well as the two additional dimensions of particulate fractions, including particles in the 1.2 µm–5 µm range and particles larger than 5 µm.

In two sampling campaigns (February and July 2019), an additional fluorescence analysis of the dissolved organic matter was performed. The results were already published as a part of the study of organic matter dynamics in the estuary [30], and data from the studied site are here used for the correlation with metal concentrations in the dissolved phase. The procedure of fluorescence analysis is described in detail in Marcinek et al., 2020 [30]. Briefly, fluorescence excitation-emission matrices were recorded using the Aqualog (Horiba-Jobin Yvon, Piscataway, NJ, USA) spectrofluorometer in a 1×1 cm^2 quartz cuvette. The scan was performed in the excitation wavelength range of 250–450 nm, with 5 nm increments, and the emission wavelength range of 220–620 nm, with 3 nm increments. The fluorescence intensity was normalized to Raman units (R.U.) using the daily-measured Raman peak of MilliQ water (λ_{ex} = 350 nm, λ_{em} = 371–428 nm). Parallel factor analysis (PARAFAC) was applied to identify the different fluorescent components by using the drEEM toolbox (version 0.2.0 for MATLAB (R2016a) [38]. Validated fluorescent components were identified by comparison with similar components reported in the literature and matching spectra obtained from the OpenFluor database [39].

3. Results and Discussion

3.1. Total Metal Concentrations Distribution within the Water Column

Before analyzing the distribution of trace metals between various fractions, it is useful to analyze their total concentrations in order to obtain a general overview of the trace metal distributions within the water column over different seasons. Vertical profiles of the total trace metal concentrations (unfiltered sample) are shown in Figure 1. Accompanying vertical salinity profiles during the time of each sampling are given in the Supplementary Materials (Figure S1). Additionally, the metal concentrations in unfiltered and filtered samples using all four cut-offs (5, 1.2, 0.1 µm and 3 kDa) in relation to salinity are given in Figures S2–S6. The highest concentration in all the samples using all filter cut-offs was determined for Al, followed by Fe, Mn, Cu/Zn, Ni, Cd/Co and Pb. Obtained concentrations were within the expected ranges and agreed well with the levels reported in previous studies from this area [8,27,29,40,41]. Concentrations of Zn, Co, Mn, Fe and Al were higher in the freshwater layer (FWL) than in the seawater layer (SWL), particularly during the winter sampling characterized by high river flow [30], indicating a dominant river source of these metals to the estuary. Conversely, concentrations of Cd, Pb and Ni generally increased from the FWL to the SWL, showing a diluting effect of the Krka River on their concentrations, as already observed for these metals in a previous study covering longitudinal estuarine transect [8]. Concentrations of Cu in the FWL changed between seasons depending on the nautical tourism activity, which is common for this estuary [8,31]. Similar Cu concentrations were observed in the FWL and SWL in non-touristic periods (February 2019 and April 2021), in contrast to summer samplings when 2–4 times higher Cu concentrations were measured in the samples from the FWL. In all the seasons, Cu showed an increase in the freshwater-seawater interface (FSI), a behavior that has already been observed in this estuary [29,35]. The accumulation in the FSI was observed also for Zn, Cd and Pb, whereas the concentration of Ni, Co, Fe and Al changed proportionally with the salinity (Figure S2). For Mn, an increase in the FSI was observed in most of the sampling campaigns (except in July 2019), as was observed in a previous study in this estuary [40]. For most of the metals, a similar relationship with salinity was observed in all filter cut-offs (Figures S2–S6). The notable difference in distributions over the salinity gradient between fractions was observed only for Pb, Mn, Fe and Al in the dissolved fraction. Namely, in contrast to higher size fractions (Figures S2–S4), concentrations of Mn,

Fe and Al in the dissolved and truly dissolved fractions increased with salinity (Figures S5 and S6). Additionally, all four metals showed a decline from the conservative behavior in the FSI only in these two fractions, indicating a precipitation and colloidal aggregation in the surface layers and their partial dissolution in the SWL.

3.2. Trace Metal Partitioning into Different Size Fractions

The average percentages of the trace metals (all sampling campaigns) in each fraction at each depth (M1–M6) are shown in Figure 2. Nickel, Cd, Zn, Co and Cu were mainly found in the truly dissolved fraction (<3 kDa), which accounted for up to 89%, 88%, 79%, 70% and 63% of their total concentrations, respectively. In contrast to these metals, the 'particulate' fractions (>0.1 µm) of Fe, Al and Pb dominated their size speciation with, on average, 84%, 75% and 51%, respectively (Table 1). Around 50% of Mn in the upper layers was present in particles, whereas in the SWL, the truly dissolved fraction dominated its size fractionation, making up to 70% of the total Mn concertation. Within the particulate fraction, these four metals were found mostly in the highest fraction (>5 µm), which corresponded to up to 67%, 59%, 44% and 40% of the total Fe, Al, Pb and Mn, respectively. Similarly, a decrease of the particulate fraction in the order Fe < Mn < Pb < Co < Zn < Cd < Cu < Ni was found in Galveston Bay [10] and Narragansett Bay [42].

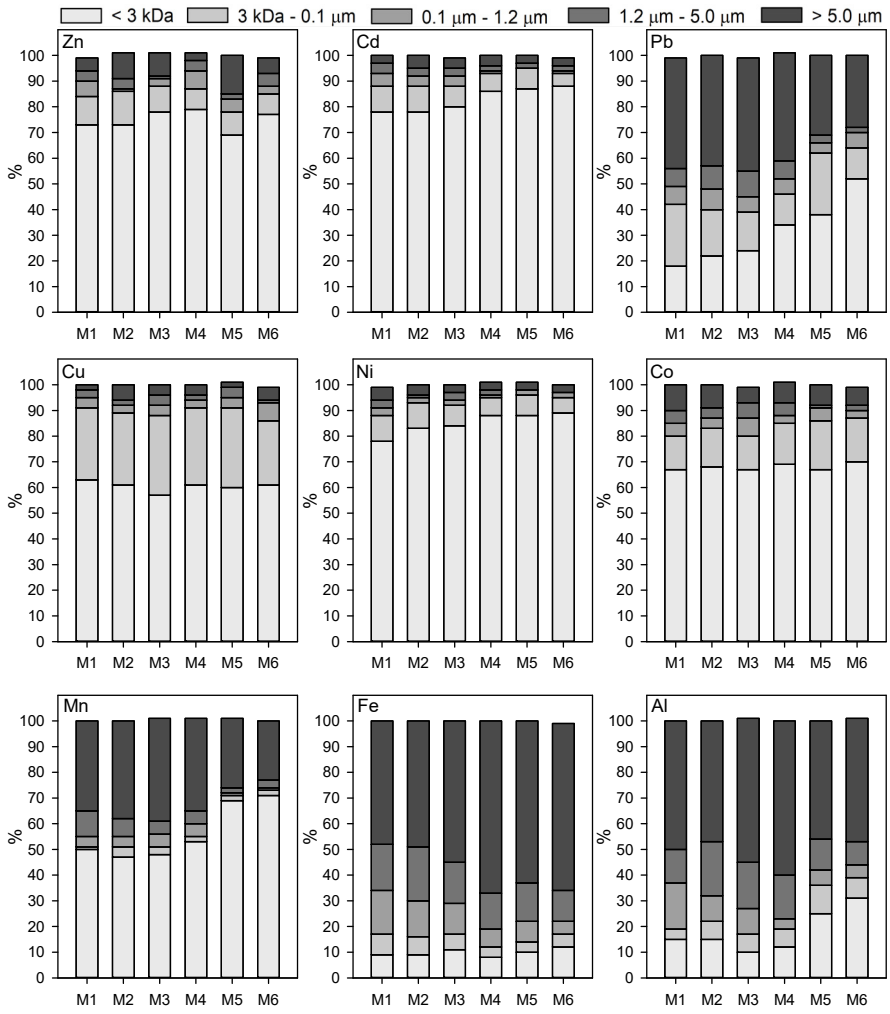

Figure 2. Average percentages of the studied trace metals (all sampling campaigns) in each size fraction (as indicated in the figure) at each depth (M1–M6).

Table 1. Average percentages of (A) particulate (>0.1 µm) and (B) colloidal (3 kDa–0.1 µm) trace metals in the total metal pool (unfiltered sample) and (C) percentages of colloidal trace metals in the dissolved metal pool (<0.1 µm).

Zn	Cd	Pb	Cu	Ni	Co	Mn	Fe	Al
(A) Average % of particulate fraction in total fraction								
15%	9%	51%	11%	7%	17%	42%	84%	75%
(B) Average % of colloidal fraction in total fraction								
10%	8%	17%	29%	8%	15%	2%	6%	7%
(C) Average % of colloidal fraction in dissolved fraction								
12%	9%	37%	32%	9%	18%	4%	37%	31%

The colloidal fraction between 3 kDa and 0.1 µm did not dominate the size speciation for any studied metal, although notable amounts of Cu, Pb and Co were found in this size range, comprising up to 31%, 24% and 19% of their total fractions, suggesting a possible influence of colloidal fraction on the migration of Cu, Pb and Co through the water column. Percentages of all studied metals, except Fe and Al, in the 0.1 µm–1.2 µm fraction, were below 6%; thus, for these metals, the formation of colloids in the 0.1 µm–1.2 µm size range was negligeable. However, Fe and Al were more abundant in this size range (up to 17% and 18% of the total fraction, respectively) than in the 3 kDa–0.1 µm range, indicating that colloidal material larger than 0.1 µm may dominate the forms of Fe and Al in the colloidal phase due to colloidal aggregation [5].

3.3. Variation in Size Distribution between Stratified Layers

For most metals (Cd, Pb, Ni, Mn, Fe, Al), an increase of the truly dissolved fraction from FWL (M1 and M2) to SWL (M5 and M6) was observed (Figure 2). For Cd, an increase of the truly dissolved species with salinity is usually ascribed to the competitive effect of chloride ions causing its release from particles [8,11]. For Pb, Mn, Fe and Al, an increase of the >5 µm size fraction was observed in the FSI (M2 and M3), indicating a close association of these metals. A transfer of metals from the low size fractions into particles in the FSI could occur via colloidal aggregation [5]. Fe and Mn may be the main carriers of Pb, and the behavior of Pb in the salinity gradient may be controlled to a significant extent by their aggregation in the mid-salinity region [6,24], indicated here by a decrease of their dissolved and truly dissolved concentrations and an increase of abundance of their high size fractions (Figure 2, Supplementary Materials Figures S5 and S6). This is consistent with a previous study that showed that the Pb distribution in the Krka estuary might be controlled by Mn and Fe particulate forms [8,26]. Fe and Mn oxides are known scavengers of various risk elements, such as Pb here. However, while cleaning the water column, they settle in the sediment and can increase the enrichment factors of these elements, which could finally mask or distort the anthropogenic contamination signals in sediment composition.

In the SWL, the particulate fractions of Pb, Mn, Fe and Al again decreased, suggesting that low size metal species are being released in response to particle desorption and the deflocculation of colloids at high salinity; a similar behavior was observed for Mn, Fe and Al in the San Francisco Bay [5]. In contrast to other metals, Zn showed an increase of the truly dissolved fraction in the FSI, whereas in the SWL, a decrease of the truly dissolved fraction along with an increase of the highest size fraction (>5 µm) was prominent. A significant decrease of the dissolved Zn fraction at high salinity was observed also by Oursel et al., 2013 [14] in a small Mediterranean river mouth. Oursel et al., 2013 [14] also observed a release of Co from particles in the mixing zone, and the same was found in the Hudson River estuary, San Francisco Bay [43] and two Japanese estuaries [44]. In the Krka estuary, Co showed a uniform distribution of its truly dissolved fraction and a decrease of the particulate fraction with salinity (21–13%), coupled with an increase of the colloidal fraction (13–19%). A much higher increase of colloidal Cd with salinity was observed in the Gulf of Trieste [37]. Finally, Cu was the only metal that showed an increase of the contribution of colloids to its dissolved fraction in the FSI. This could be due to the binding

with biologically-produced organic ligands, such as colloidally-associated thiols or other cluster forming sulfide complexes [10,45], since, according to previous studies, the highest biological activity in the estuary is associated with the FSI [32,46,47].

The salinity of the surface FWL differed between sampling campaigns depending on the Krka River flow; thus, the averaged trace metal fractions were also calculated separately for campaigns characterized by the salinity of FWL <25 (February 2019, July 2019, April 2021) (Figure S7) and >25 (July 2018, July 2020, September 2020) (Figure S8). As expected, the size distribution of metals in the SWL was very similar in both periods, while in the FWL and FSI, slight differences were observed between low and high salinity periods, namely for metals with a dominant river source (Zn, Co, Mn, Fe and Al) and Pb, as it is evidently associated with Mn, Fe and Al in the estuary. In low salinity periods, i.e., higher river flow periods, the concentration of these metals in the three middle fractions (3 kDa–5 µm) was much higher compared to high salinity periods, meaning that these metals are introduced by the river mostly in this size range. An increased concentration of the highest fraction (>5 µm) for Pb, Mn, Fe and Al during the high salinity period can be explained with an increased contribution of atmospheric deposition during low river flow [48].

3.4. Significance of Colloidal Metal Fraction in the Dissolved Phase-Comparison with Other Coastal Areas

3.4.1. Metals with High Particulate Reactivity (Pb, Mn, Fe, Al)

For metals that were present primarily in the particulate fraction, a high percentage of colloids was found in the dissolved fraction as well (37%, 37% and 31% for Pb, Fe and Al, respectively) (Table 1). Similarly to Pb in the Krka River estuary, on average, 30% of dissolved Pb was present in the colloidal fraction in the Guandang River estuary [24] and the coast of the North Yellow Sea [22], in contrast to the Xin'an River estuary, with <14% of colloidal Pb in the dissolved pool [24] (Table S1). In other studies, the colloidal fraction dominated Pb concentration in the dissolved pool, with much higher percentages than in the Krka River estuary, such as in the Penzé estuary [6] or Galveston Bay [49], where colloidal (5 kDa–0.2 µm and 10 kDa–0.4 µm, respectively) Pb accounted for most of the dissolved metal (>94%). In other coastal areas, much higher or much lower colloidal Fe and Al were found compared to our study (Table S1). For example, in Venice Lagoon, colloidal Fe (100 kDa–0.4 µm) accounted for 87% of the dissolved fraction [50], whereas in the Gulf of Trieste, colloidal Fe and Al (5 kDa–0.2 µm) averaged only 7.6% and 1.5%, respectively [37]. In San Francisco Bay, >84% of dissolved Fe and Al was associated with colloidal material (10 kDa–0.2 µm) in the low salinity region, while at high salinities, colloidal Fe was still high (40%), but very little colloidal Al was detected [5]. In contrast to Pb, Fe and Al, Mn showed the lowest colloidal reactivity among all the studied metals, with only 4% of colloidal Mn present in the dissolved phase. Similarly, <20%, i.e., <10% in the high-salinity region, of colloidal Mn was found in San Francisco Bay [5] and the Gulf of Trieste [37] (Table S1).

3.4.2. Metals Associated with Dissolved Organic Matter (Cu, Co)

When considering the total metal fraction, Cu showed the highest affinity to colloids among studied metals. In the total fraction, on average, 29% of Cu was present as colloidal compounds, which is considerably more than for other studied metals (Table 1). Unlike Pb, Fe and Al, which relied on both the colloidal and particulate fraction, a small amount of Cu was bound to >0.1 µm particles (<11%), highlighting the importance of the colloidal fraction to Cu distribution in the estuary. In the dissolved fraction, on average, 32% of Cu was present as colloidal compounds, similar to the results obtained in the Gulf of Trieste [37] and Loire estuary [51]. When comparing the importance of colloidal Cu in various estuarine systems, disparate results are obtained (Table S1). In the Xin'an River, Guandang River estuaries [24] and San Francisco Bay [5], 86–92% of dissolved Cu was found in the truly dissolved phase, whereas in the Penzé estuary [6], Ob estuary [52] and Fal estuary [11], the colloidal fraction dominated the Cu size speciation. Cu complexes with dissolved organic

ligands have been widely reported to dominate the Cu speciation in the dissolved fraction, so the differences in its size distribution between different studies could be related to differences in the organic matter composition within these systems [51,53–56]. A competition between high and low molecular weight organic ligands could drive the Cu size distribution in estuarine systems [10], such as the increase of colloidal Cu in the FSI observed in our study (Figure 2). Tang et al., 2001 [57] showed that, in Galveston Bay, colloidal Cu-binding ligands have, on average, 60 times higher conditional stability constants than truly dissolved ligands. Similarly, in the Loire estuary, the colloidal Cu-binding ligands were estimated to be 4 to 260 times stronger than those found in the truly dissolved phase [51]. In coastal waters, macromolecular Cu-binding ligands in the colloidal size range could be allochthonous humic aggregates or freshly produced high molecular weight biomolecules, such as proteins or polysaccharides [6]. In the Krka estuary, the dissolved Cu concentration showed the highest correlation with protein-like (tryptophan-like) fluorescent substances (Figure 3A) (PARAFAC component C3: $\lambda_{ex}/\lambda_{em}$ = 275/344; detailed in Marcinek et al., 2020 [30]). Protein-like fluorophores are considered to be derived from freshly produced autochthonous organic matter and showed an evident relationship with elevated biological activity [58,59]. Similarly to the Krka estuary, in the Gulf of Trieste, among 13 analyzed metals (including Mn, Fe, Co, Ni, Zn, Cd and Pb), Cu (along with Hg) showed the highest affinity to colloidal organic matter that mostly originated from phytoplankton activity [37]. Proteinaceous substances bear sulfur functional groups that strongly bind Cu; thus, they can play a major role in the estuarine Cu biogeochemistry [56,60]. Biogenic reduced sulfur species can also enhance the formation of polysaccharide aggregates and Cu uptake into the colloidal fraction [10,61]. In the Galveston Bay, colloidal Cu-organic complexes mediate the partitioning between particles and solution [57]. In this system, reduced sulfur species from biological sources accounted for most of the Cu-complexing ligands [57]. In addition, in the Loire estuary, proteinaceous colloidal material was most likely the cause of the change of Cu speciation in the middle of the estuary [51].

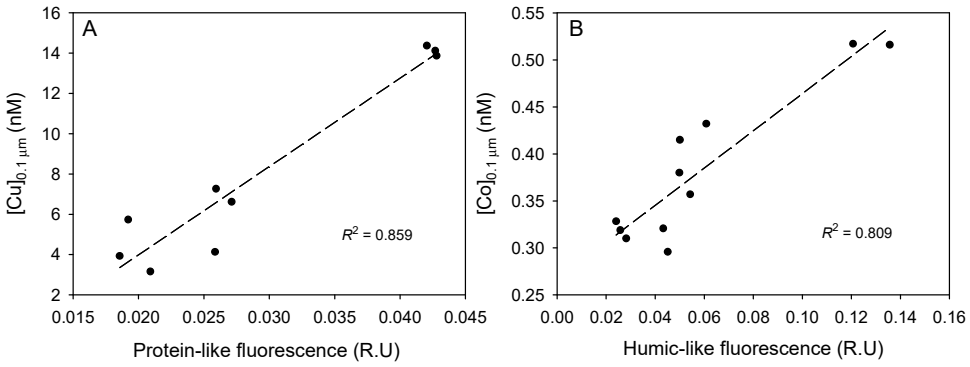

Figure 3. Correlation of (**A**) dissolved Cu with protein-like PARAFAC components, and (**B**) dissolved Co with humic-like PARAFAC components.

On average, 18% of Co in the dissolved fraction was associated with colloids (Table 1), similar to Galveston Bay where the colloidal fraction (1 kDa–0.45 µm) averaged 19% of the filter-passing pool [62] (Table S1). In the Amazon and Pará River estuaries, on the other hand, up to 86% of colloidal Co (0.015–0.2 µm) was found in the dissolved fraction in the low-salinity range and, in contrast to the Krka River estuary, showed a general decrease, with salinity down to 16% [63]. In the Amazon and Pará River estuaries, reactive dissolved Co was absent, indicating the presence of strong organic Co complexes. Interestingly, in the Krka River estuary, Co was the only metal that showed a strong association with humic-like fluorescent substances (Figure 3B) (PARAFAC components C1 + C2: $\lambda_{ex}/\lambda_{em}$ = 305/416 and $\lambda_{ex}/\lambda_{em}$ = 275 (345)/479, respectively; detailed in Marcinek et al., 2020 [30]). Co complexation with humic material was also found in the South Bay of the San Francisco Estuary [64]. A previous study of organic matter in the Krka River estuary [30] showed

that humic-like fluorescent compounds behave conservatively in the horizontal salinity gradient, similar to dissolved Co's behavior in the vertical salinity gradient observed here (Figure S4), in contrast to protein-like fluorescence, which was higher than expected by linear mixing at mid-salinity range, similar to the Cu behavior observed in this study.

3.4.3. Metals with Small Colloidal and Particulate Fractions (Zn, Cd, Ni)

Small amounts of colloidal Zn, Cd and Ni were detectable, with, on average, 9%, 9% and 12% in the dissolved phase, respectively (Table 1). In other studies, even lower amounts of colloidal Zn, Cd and Ni were detectable than in the Krka River estuary (Table S1), such as in the Gulf of Trieste [37] and San Francisco Bay [5], where more than 96% of Zn and Ni and more than 99% of Cd was present in the truly dissolved phase (<5 kDa and <10 kDa, respectively). In Galveston Bay, on the contrary, Zn had almost no truly dissolved fraction (averaging 9%), and colloidal Ni (1 kDa–0.45 um) was much higher, averaging 36% of the filter-passing pool [62]. In the Amazon and Pará River estuaries, dissolved Ni was present mostly in the 'reactive' form, suggesting high bioavailability, and colloidal Ni (0.015–0.2 µm) was only detected at salinity <28 (up to 38%). Similarly to the Krka River estuary, <12% of colloidal Cd was found in the Xin'an River and Guandang River estuaries [24]. In contrast, a much higher percentage of colloidal Cd in the dissolved fraction was found in most of the other coastal systems, e.g., Venice Lagoon [50], Fal estuary [11], the coastal waters of North Yellow Sea [22], Galveston Bay [62] and Penzé estuary [6], with on average 34%, 37%, 38%, 44% and even 82% of colloidal Cd, respectively.

4. Conclusions

This study was aimed at quantitatively assessing the size distribution of various trace metals (Zn, Cd, Pb, Cu, Ni, Co, Mn, Fe and Al) in the vertical salinity gradient of the highly stratified Krka River estuary, which is characterized by a low riverine input of trace elements, suspended particulate matter and organic carbon. The particularity of this study was the distribution of size fractions, which spanned ~5 orders of magnitude ranging from >5 µm to <3 kDa. Overall, the dominant river source was indicated for Zn, Co, Mn, Fe and Al, while the river showed a diluting effect on the concentration of Cd, Pb and Ni in the estuary. The truly dissolved fraction (<3 kDa) dominated the Zn (75%), Cd (83%), Cu (60%), Ni (85%), Co (68%) and Mn (56%) fractionation, while Pb, Fe and Al were mainly present in a particulate form larger than 0.1 µm (56, 85 and 75%, respectively). Although the truly dissolved fraction dominated the Mn fractionation, the fraction between 3 kDa and 5 µm accounted for less than 10% on average, indicating the preferential formation of larger Mn particles under estuarine conditions.

Colloids, as a subgroup of the dissolved fraction, represented a small absolute fraction for all elements. However, their contribution to the dissolved pool was relatively high for Pb (37%), Cu (32%), Fe (37%) and Al (31%), indicating a significant contribution of high molecular weight forms. High molecular weight forms can be formed by biologically-produced organic ligands (such as reduced sulfur species), which was evident for Cu that correlated well with protein-like organic compounds. Interestingly, Co was the only metal that showed a strong association with humic-like substances in the dissolved phase.

The comparison with other studies showed inconsistent results, suggesting that various environmental factors, such as chemical composition and the flux of organic matter and suspended particles, play a crucial role in defining the fractionation of trace metals in estuarine systems. In order to qualitatively resolve the observed quantitative distributions of size fractionation/species and fate of trace metals in the Krka River estuary, a more focused and detailed study encompassing the entire horizontal estuarine transect is required.

Supplementary Materials: The following are available online at https://www.mdpi.com/article/10.3390/app12125816/s1, Figure S1: Vertical salinity profiles during the time of the samplings, Figure S2: Concentrations of studied trace metals in the total fraction (unfiltered sample) in relation to salinity, Figure S3: Concentrations of studied trace metals in <5 μM fraction in relation to salinity, Figure S4: Concentrations of studied trace metals in <1.2 μM fraction in relation to salinity, Figure S5: Concentrations of studied trace metals in <0.1 μM fraction in relation to salinity, Figure S6. Concentrations of studied trace metals in truly dissolved fraction (<3 kDa) in relation to salinity, Figure S7: Average percentages of studied trace metals (samplings with FWL characterised by salinity <25) in each size fraction at each depth (M1–M6); Figure S8. Average percentages of studied trace metals (samplings with FWL characterised by salinity >25) in each size fraction at each depth (M1–M6). Table S1: Percentage of colloidal metal fraction in the dissolved phase - comparison between various coastal areas.

Author Contributions: Conceptualization, S.M. and D.O.; methodology, A.M.C. and J.P.; validation, A.M.C. and J.P.; formal analysis, S.M., A.M.C. and J.P.; investigation, S.M., A.M.C. and J.P.; resources, D.O.; data curation, S.M.; writing—original draft preparation, S.M.; writing—review and editing, S.M., A.M.C., J.P. and D.O.; visualization, S.M. and D.O.; supervision, D.O.; project administration, D.O.; funding acquisition, D.O. All authors have read and agreed to the published version of the manuscript.

Funding: This research was realized within the framework of the project 'New methodological approach to biogeochemical studies of trace metal speciation in coastal aquatic ecosystems (MEBTRACE)' (IP-2014-09-7530-MEBTRACE) funded by the Croatian Science Foundation.

Institutional Review Board Statement: Not applicable.

Informed Consent Statement: Not applicable.

Data Availability Statement: The data presented in this study are available upon request from the corresponding authors.

Conflicts of Interest: The authors declare no conflict of interest.

References

1. Lead, J.R.; Wilkinson, K.J. Environmental Colloids and Particles: Current Knowledge and Future Developments. In *Environmental Colloids and Particles: Behaviour, Separation and Characterisation*; Wilkinson, K.J., Lead, J.R., Eds.; John Wiley & Sons, Ltd.: Chichester, UK, 2007; pp. 1–15.
2. Wells, M.L. Marine Colloids and Trace Metals. In *Biogeochemistry of Marine Dissolved Organic Matter*; Hansell, D.A., Carlson, C.A., Eds.; Academic Press: Cambridge, MA, USA, 2002; pp. 367–404, ISBN 9780124059405.
3. Filella, M. Colloidal Properties of Submicron Particles in Natural Waters. In *Environmental Colloids and Particles: Behaviour, Separation and Characterisation*; Wilkinson, K.J., Lead, J.R., Eds.; John Wiley & Sons, Ltd.: Chichester, UK, 2007; pp. 6, 17–93, ISBN 9780470024539.
4. Everett, D.H. Manual of Symbols and Terminology for Physicochemical Quantities and Units, Appendix II: Definitions, Terminology and Symbols in Colloid and Surface Chemistry. *Pure Appl. Chem.* **1972**, *31*, 577–638. [CrossRef]
5. Sañudo-Wilhelmy, S.A.; Rivera-Duarte, I.; Flegal, A.R. Distribution of colloidal trace metals in the San Francisco Bay estuary. *Geochim. Cosmochim. Acta* **1996**, *60*, 4933–4944. [CrossRef]
6. Waeles, M.; Tanguy, V.; Lespes, G.; Riso, R.D. Behaviour of colloidal trace metals (Cu, Pb and Cd) in estuarine waters: An approach using frontal ultrafiltration (UF) and stripping chronopotentiometric methods (SCP). *Estuarine Coast. Shelf Sci.* **2008**, *80*, 538–544. [CrossRef]
7. Santschi, P.H.; Lenhart, J.J.; Honeyman, B.D. Heterogeneous processes affecting trace contaminant distribution in estuaries: The role of natural organic matter. *Mar. Chem.* **1997**, *58*, 99–125. [CrossRef]
8. Cindric, A.-M.; Garnier, C.; Oursel, B.; Pižeta, I.; Omanović, D. Evidencing the natural and anthropogenic processes controlling trace metals dynamic in a highly stratified estuary: The Krka River estuary (Adriatic, Croatia). *Mar. Pollut. Bull.* **2015**, *94*, 199–216. [CrossRef]
9. Wang, W.; Chen, M.; Guo, L.; Wang, W.-X. Size partitioning and mixing behavior of trace metals and dissolved organic matter in a South China estuary. *Sci. Total Environ.* **2017**, *603–604*, 434–444. [CrossRef]
10. Tang, D.; Warnken, K.W.; Santschi, P.H. Distribution and partitioning of trace metals (Cd, Cu, Ni, Pb, Zn) in Galveston Bay waters. *Mar. Chem.* **2002**, *78*, 29–45. [CrossRef]
11. Braungardt, C.B.; Howell, K.A.; Tappin, A.D.; Achterberg, E.P. Temporal variability in dynamic and colloidal metal fractions determined by high resolution in situ measurements in a UK estuary. *Chemosphere* **2011**, *84*, 423–431. [CrossRef]

12. Tercier-Waeber, M.L.; Stoll, S.; Slaveykova, V.I. Trace Metal Behavior in Surface Waters: Emphasis on Dynamic Spéciation, Sorption Processes and Bioavailability. *Arch. Sci.* **2012**, *65*, 119–142.
13. Tanguy, V.; Waeles, M.; Gigault, J.; Cabon, J.-Y.; Quentel, F.; Riso, R.D. The removal of colloidal lead during estuarine mixing: Seasonal variations and importance of iron oxides and humic substances. *Mar. Freshw. Res.* **2011**, *62*, 329–341. [CrossRef]
14. Oursel, B.; Garnier, C.; Durrieu, G.; Mounier, S.; Omanović, D.; Lucas, Y. Dynamics and fates of trace metals chronically input in a Mediterranean coastal zone impacted by a large urban area. *Mar. Pollut. Bull.* **2013**, *69*, 137–149. [CrossRef]
15. Waeles, M.; Tanguy, V.; Riso, R.D. On the control of copper colloidal distribution by humic substances in the Penzé estuary. *Chemosphere* **2015**, *119*, 1176–1184. [CrossRef]
16. De Souza Machado, A.A.; Spencer, K.; Kloas, W.; Toffolon, M.; Zarfl, C. Metal fate and effects in estuaries: A review and conceptual model for better understanding of toxicity. *Sci. Total Environ.* **2016**, *541*, 268–281. [CrossRef]
17. Cobelo-García, A.; Prego, R. Land inputs, behaviour and contamination levels of copper in a ria estuary (NW Spain). *Mar. Environ. Res.* **2003**, *56*, 403–422. [CrossRef]
18. Muller, F. Interactions of copper, lead and cadmium with the dissolved, colloidal and particulate components of estuarine and coastal waters. *Mar. Chem.* **1996**, *52*, 245–268. [CrossRef]
19. Jiann, K.-T.; Wen, L.-S.; Santschi, P.H. Trace metal (Cd, Cu, Ni and Pb) partitioning, affinities and removal in the Danshuei River estuary, a macro-tidal, temporally anoxic estuary in Taiwan. *Mar. Chem.* **2005**, *96*, 293–313. [CrossRef]
20. Batchelli, S.; Muller, F.L.; Baalousha, M.; Lead, J.R. Size fractionation and optical properties of colloids in an organic-rich estuary (Thurso, UK). *Mar. Chem.* **2009**, *113*, 227–237. [CrossRef]
21. Fang, Z.; Wang, W.-X. Size speciation of dissolved trace metals in hydrothermal plumes on the Southwest Indian Ridge. *Sci. Total Environ.* **2021**, *771*, 145367. [CrossRef]
22. Lu, Y.; Gao, X.; Chen, C.-T.A. Separation and determination of colloidal trace metals in seawater by cross-flow ultrafiltration, liquid-liquid extraction and ICP-MS. *Mar. Chem.* **2019**, *215*, 103685. [CrossRef]
23. Schlosser, C.; Streu, P.; Croot, P.L. Vivaspin ultrafiltration: A new approach for high resolution measurements of colloidal and soluble iron species. *Limnol. Oceanogr. Methods* **2013**, *11*, 187–201. [CrossRef]
24. Lu, Y.; Gao, X.; Song, J.; Chen, C.-T.A.; Chu, J. Colloidal toxic trace metals in urban riverine and estuarine waters of Yantai City, southern coast of North Yellow Sea. *Sci. Total Environ.* **2019**, *717*, 135265. [CrossRef]
25. Scribe, P.; Fillaux, J.; Laureillard, J.; Denant, V.; Saliot, A. Fatty acids as biomarkers of planktonic inputs in the stratified estuary of the Krka River, Adriatic Sea: Relationship with pigments. *Mar. Chem.* **1991**, *32*, 299–312. [CrossRef]
26. Cukrov, N.; Frančišković-Bilinski, S.; Mikac, N.; Roje, V. Natural and Anthropogenic Influences Recorded in Sediments from the Krka River Estuary (Eastern Adriatic Coast), Evaluated by Statistical Methods. *Fresenius Environ. Bull.* **2008**, *17*, 855–863.
27. Pađan, J.; Marcinek, S.; Cindrić, A.-M.; Layglon, N.; Lenoble, V.; Salaün, P.; Garnier, C.; Omanović, D. Improved voltammetric methodology for chromium redox speciation in estuarine waters. *Anal. Chim. Acta* **2019**, *1089*, 40–47. [CrossRef]
28. Pađan, J.; Marcinek, S.; Cindrić, A.-M.; Layglon, N.; Garnier, C.; Salaün, P.; Cobelo-Garcia, A.; Omanović, D. Determination of sub-picomolar levels of platinum in the pristine Krka River estuary (Croatia) using improved voltammetric methodology. *Environ. Chem.* **2020**, *17*, 77. [CrossRef]
29. Cindrić, A.-M.; Marcinek, S.; Garnier, C.; Salaün, P.; Cukrov, N.; Oursel, B.; Lenoble, V.; Omanović, D. Evaluation of diffusive gradients in thin films (DGT) technique for speciation of trace metals in estuarine waters—A multimethodological approach. *Sci. Total Environ.* **2020**, *721*, 137784. [CrossRef]
30. Marcinek, S.; Santinelli, C.; Cindrić, A.-M.; Evangelista, V.; Gonnelli, M.; Layglon, N.; Mounier, S.; Lenoble, V.; Omanović, D. Dissolved organic matter dynamics in the pristine Krka River estuary (Croatia). *Mar. Chem.* **2020**, *225*, 103848. [CrossRef]
31. Carić, H.; Cukrov, N.; Omanović, D. Nautical Tourism in Marine Protected Areas (MPAs): Evaluating an Impact of Copper Emission from Antifouling Coating. *Sustainability* **2021**, *13*, 11897. [CrossRef]
32. Viličić, D.; Legović, T.; Žutić, V. Vertical distribution of phytoplankton in a stratified estuary. *Aquat. Sci.* **1989**, *51*, 31–46. [CrossRef]
33. Sempéré, R.; Cauwet, G. Occurrence of organic colloids in the stratified estuary of the Krka River (Croatia). *Estuarine Coast. Shelf Sci.* **1995**, *40*, 105–114. [CrossRef]
34. Bilinski, H. Mercury distribution in the water column of the stratified Krka river estuary (Croatia): Importance of natural organic matter and of strong winds. *Water Res.* **2000**, *34*, 2001–2010. [CrossRef]
35. Louis, Y.; Garnier, C.; Lenoble, V.; Mounier, S.; Cukrov, N.; Omanović, D.; Pižeta, I. Kinetic and equilibrium studies of copper-dissolved organic matter complexation in water column of the stratified Krka River estuary (Croatia). *Mar. Chem.* **2009**, *114*, 110–119. [CrossRef]
36. Karanfil, T.; Erdogan, I.; Schlautman, M.A. Selecting Filter Membranes for measuring DOC and UV_{254}. *J. Am. Water Work. Assoc.* **2003**, *95*, 86–100. [CrossRef]
37. Klun, K.; Falnoga, I.; Mazej, D.; Šket, P.; Faganeli, J. Colloidal Organic Matter and Metal(loid)s in Coastal Waters (Gulf of Trieste, Northern Adriatic Sea). *Aquat. Geochem.* **2019**, *25*, 179–194. [CrossRef]
38. Murphy, K.R.; Stedmon, C.A.; Graeber, D.; Bro, R. Fluorescence spectroscopy and multi-way techniques. PARAFAC. *Anal. Methods* **2013**, *5*, 6557–6566. [CrossRef]
39. Murphy, K.R.; Stedmon, C.A.; Wenig, P.; Bro, R. OpenFluor—An online spectral library of auto-fluorescence by organic compounds in the environment. *Anal. Methods* **2013**, *6*, 658–661. [CrossRef]

40. Omanović, D.; Kwokal, Ž.; Goodwin, A.; Lawrence, A.; Banks, C.E.; Compton, R.G.; Komorsky-Lovrić, Š. Trace metal detection in Šibenik Bay, Croatia: Cadmium, lead and copper with anodic stripping voltammetry and manganese via sonoelectrochemistry. A case study. *J. Iran. Chem. Soc.* **2006**, *3*, 128–139. [CrossRef]
41. Penezić, A.; Milinković, A.; Alempijević, S.B.; Žužul, S.; Frka, S. Atmospheric deposition of biologically relevant trace metals in the eastern Adriatic coastal area. *Chemosphere* **2021**, *283*, 131178. [CrossRef]
42. Wells, M.L.; Smith, G.J.; Bruland, K. The distribution of colloidal and particulate bioactive metals in Narragansett Bay, RI. *Mar. Chem.* **2000**, *71*, 143–163. [CrossRef]
43. Tovar-Sánchez, A.; Sañudo-Wilhelmy, S.A.; Flegal, A. Temporal and spatial variations in the biogeochemical cycling of cobalt in two urban estuaries: Hudson River Estuary and San Francisco Bay. *Estuarine Coast. Shelf Sci.* **2004**, *60*, 717–728. [CrossRef]
44. Takata, H.; Aono, T.; Tagami, K.; Uchida, S. Processes controlling cobalt distribution in two temperate estuaries, Sagami Bay and Wakasa Bay, Japan. *Estuarine Coast. Shelf Sci.* **2010**, *89*, 294–305. [CrossRef]
45. Rozan, T.F.; Lassman, M.E.; Ridge, D.P.; Luther, G.W. Evidence for iron, copper and zinc complexation as multinuclear sulphide clusters in oxic rivers. *Nature* **2000**, *406*, 879–882. [CrossRef]
46. Svensen, C.; Viličić, D.; Wassmann, P.; Arashkevich, E.; Ratkova, T. Plankton distribution and vertical flux of biogenic matter during high summer stratification in the Krka estuary (Eastern Adriatic). *Estuarine Coast. Shelf Sci.* **2007**, *71*, 381–390. [CrossRef]
47. Cetinić, I.; Viličić, D.; Burić, Z.; Olujić, G. Phytoplankton Seasonality in a Highly Stratified Karstic Estuary (Krka, Adriatic Sea). *Hydrobiologia* **2006**, *555*, 31–40. [CrossRef]
48. Guerzoni, S.; Chester, R.; Dulac, F.; Herut, B.; Loÿe-Pilot, M.-D.; Measures, C.; Migon, C.; Molinaroli, E.; Moulin, C.; Rossini, P.; et al. The role of atmospheric deposition in the biogeochemistry of the Mediterranean Sea. *Prog. Oceanogr.* **1999**, *44*, 147–190. [CrossRef]
49. Benoit, G.; Oktay-Marshall, S.; Cantu, A.; Hood, E.; Coleman, C.; Corapcioglu, M.; Santschi, P. Partitioning of Cu, Pb, Ag, Zn, Fe, Al, and Mn between filter-retained particles, colloids, and solution in six Texas estuaries. *Mar. Chem.* **1994**, *45*, 307–336. [CrossRef]
50. Martin, J.-M.; Dai, M.-H.; Cauwet, G. Significance of colloids in the biogeochemical cycling of organic carbon and trace metals in the Venice Lagoon (Italy). *Limnol. Oceanogr.* **1995**, *40*, 119–131. [CrossRef]
51. Dulaquais, G.; Waeles, M.; Breitenstein, J.; Knoery, J.; Riso, R. Links between size fractionation, chemical speciation of dissolved copper and chemical speciation of dissolved organic matter in the Loire estuary. *Environ. Chem.* **2020**, *17*, 385. [CrossRef]
52. Dai, M.-H.; Martin, J.-M. First data on trace metal level and behaviour in two major Arctic river-estuarine systems (Ob and Yenisey) and in the adjacent Kara Sea, Russia. *Earth Planet. Sci. Lett.* **1995**, *131*, 127–141. [CrossRef]
53. Sedlak, D.L.; Phinney, J.T.; Bedsworth, W.W. Strongly Complexed Cu and Ni in Wastewater Effluents and Surface Runoff. *Environ. Sci. Technol.* **1997**, *31*, 3010–3016. [CrossRef]
54. Berg, C.M.V.D.; Merks, A.G.; Duursma, E.K. Organic complexation and its control of the dissolved concentrations of copper and zinc in the Scheldt estuary. *Estuarine Coast. Shelf Sci.* **1987**, *24*, 785–797. [CrossRef]
55. Buck, K.N.; Ross, J.R.; Flegal, A.R.; Bruland, K.W. A review of total dissolved copper and its chemical speciation in San Francisco Bay, California. *Environ. Res.* **2007**, *105*, 5–19. [CrossRef]
56. Whitby, H.; Hollibaugh, J.T.; van den Berg, C.M.G. Chemical Speciation of Copper in a Salt Marsh Estuary and Bioavailability to Thaumarchaeota. *Front. Mar. Sci.* **2017**, *4*, 178. [CrossRef]
57. Tang, D.; Warnken, K.W.; Santschi, P.H. Organic complexation of copper in surface waters of Galveston Bay. *Limnol. Oceanogr.* **2001**, *46*, 321–330. [CrossRef]
58. Coble, P.G. Marine Optical Biogeochemistry: The Chemistry of Ocean Color. *Chem. Rev.* **2007**, *107*, 402–418. [CrossRef]
59. Yamashita, Y.; Tanoue, E. Chemical characterization of protein-like fluorophores in DOM in relation to aromatic amino acids. *Mar. Chem.* **2003**, *82*, 255–271. [CrossRef]
60. Laglera, L.M.; Berg, C.M.V.D. Copper complexation by thiol compounds in estuarine waters. *Mar. Chem.* **2003**, *82*, 71–89. [CrossRef]
61. Ciglenečki, I.; Ćosović, B.; Vojvodić, V.; Plavsic, M.; Furić, K.; Minacci, A.; Baldi, F. The role of reduced sulfur species in the coalescence of polysaccharides in the Adriatic Sea. *Mar. Chem.* **2000**, *71*, 233–249. [CrossRef]
62. Wen, L.-S.; Santschi, P.; Gill, G.; Paternostro, C. Estuarine trace metal distributions in Galveston Bay: Importance of colloidal forms in the speciation of the dissolved phase. *Mar. Chem.* **1999**, *63*, 185–212. [CrossRef]
63. de Carvalho, L.M.; Hollister, A.P.; Trindade, C.; Gledhill, M.; Koschinsky, A. Distribution and size fractionation of nickel and cobalt species along the Amazon estuary and mixing plume. *Mar. Chem.* **2021**, *236*, 104019. [CrossRef]
64. Ndung'u, K.; Franks, R.P.; Bruland, K.W.; Flegal, A. Organic complexation and total dissolved trace metal analysis in estuarine waters: Comparison of solvent-extraction graphite furnace atomic absorption spectrometric and chelating resin flow injection inductively coupled plasma-mass spectrometric analysis. *Anal. Chim. Acta* **2003**, *481*, 127–138. [CrossRef]